
Article:
Radhakrishnan, Vignesh, Patil, Samadhan orcid.org/0000-0002-3697-0725, Pelah, Adar orcid.org/0000-0002-9506-4685 et al. (1 more author) (2024) Influence of multibody kinematic optimisation pipeline on marker residual errors. Journal of biomechanics. 112395. ISSN 0021-9290

https://doi.org/10.1016/j.jbiomech.2024.112395

Journal of Biomechanics 177 (2024) 112395

Contents lists available at ScienceDirect

Journal of Biomechanics

journal homepage: www.elsevier.com/locate/jbiomech

Influence of multibody kinematic optimisation pipeline on marker residual errors

Vignesh Radhakrishnan *, Samadhan Patil, Adar Pelah, Peter Ellison

School of Physics, Engineering and Technology, University of York, UK

ARTICLE INFO

Keywords:
Multibody kinematic optimisation
Soft tissue artefacts
OpenSim
Inverse-kinematics
Gait analysis

ABSTRACT

Residual errors are used as a goodness-of-fit metric of the musculoskeletal model to the experimental data in multibody kinematic optimisation (MKO) analyses. Despite many studies reporting residual errors as a criterion for evaluating their proposed algorithm or model, the validity of residual errors as a performance metric has been questioned, with studies indicating a non-causal relationship between residual errors and computed joint angles. Additionally, the impact of different parameters of an MKO pipeline on residual errors has not been analysed. In our study, we have investigated the effect of each step of the MKO pipeline on residual errors, and the existence of a causal relationship between residual errors and joint angles. Increases in residual errors from the baseline model (13.84 [12.72, 15.15]mm) were obtained for: models with marker registration errors of 1.25 cm (16.36 [15.37, 17.57]mm); models with segment scaling errors of 1.25 cm (14.84 [13.77, 16.24]mm); variation in marker weighting scheme (15.28[14.00, 16.85]mm); and models with differing joint constraints (18.21[17.37, 19.11]mm). We also observed that significant variation in residual errors results in significant variation in computed joint angles, with increases in residual error positively correlated with increases in joint angle errors when the same MKO pipeline is employed. Our findings support the existence of a causal relationship and present the significant effect the MKO pipeline has on residual errors. We believe our results can further the discussion of residual errors as a goodness-of-fit metric, specifically in the absence of artefact-free bone movement.

1. Introduction

Skin-mounted marker-based systems are the gold standard for clinical movement analysis; however, the clinical usability of their data is affected by kinematic errors, which are predominantly caused by soft tissue artefacts (STA). Due to the subject-, task- and location-specific nature of STA, they are difficult to compensate for and are frequently considered the most critical source of error in movement analysis (Cappello et al., 2005; Leardini et al., 2005; Camomilla et al., 2017).

Multibody kinematic optimisation (MKO) is widely applied to reduce the effects of STA on computed kinematics (De Groote et al., 2008; Kainz et al., 2016; Lu and O'Connor, 1999), with MKO approaches implemented in commonly used musculoskeletal modelling software, such as OpenSim (Delp et al., 2007) and Anybody (Damsgaard et al., 2006). The following pipeline is commonly applied in MKO methods (Fig. 1): scaling of a generic musculoskeletal model incorporating different joint models (segment scaling), registering model-derived markers to experimental markers (marker registration) and calculating joint angles using an MKO method, with the option of altering marker weights (marker weight schemes).

Residual errors (the optimised difference between measured and model-derived skin-marker trajectories) derive from the MKO method and are often used to evaluate the MKO pipeline. For example, different scaling methods (segment scaling and marker registration) were evaluated using residual errors as a metric (Lund et al., 2015; Puchaud et al., 2020), with optimisation-based scaling reported to be more effective than linear scaling. Similarly, residual errors were leveraged to evaluate different MKO formulations (Bonnet et al., 2017b) with a constrained extended kalman filter (EKF) reported to reduce residual errors. Studies have also reported that residual errors are sensitive to the MKO method employed (Ojeda et al., 2014).

Residual errors have also been used as a goodness-of-fit metric between the underlying model and the experimental data (Begon et al., 2018). Lower residual errors have been reported as an indicator of: superior pose reconstruction capability of the proposed model (Laitenberger et al., 2015), improved STA compensation (Andersen et al., 2012) and higher accuracy in joint centre estimation (Pomarat et al., 2023). Typically, lower residual errors are indicative of lower kinematic errors, supporting the existence of a causal relationship

* Corresponding author.
E-mail address: vignesh.radhakrishnan@york.ac.uk (V. Radhakrishnan).

https://doi.org/10.1016/j.jbiomech.2024.112395
Accepted 24 October 2024
Available online 1 November 2024

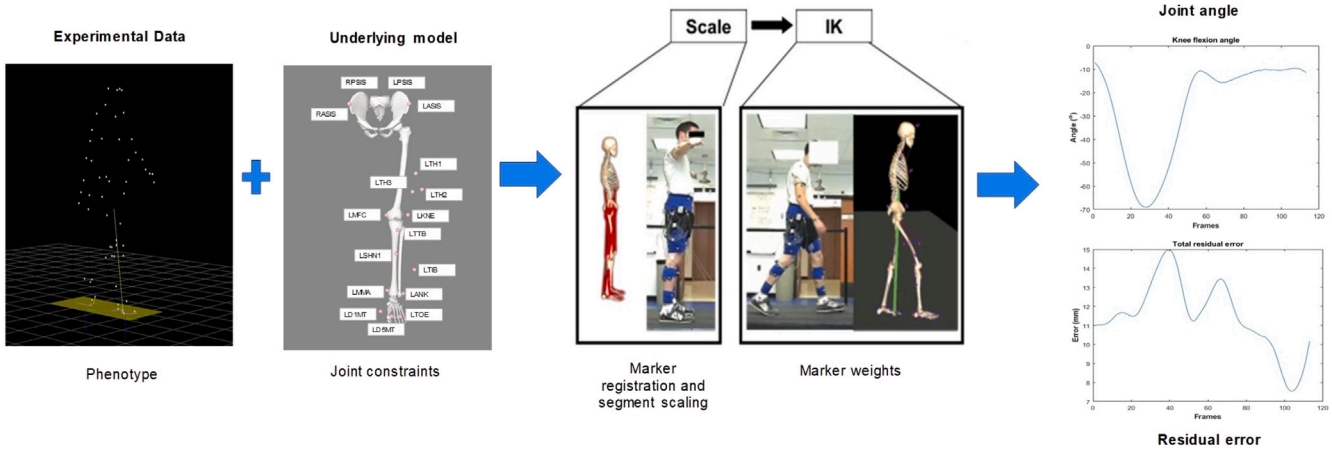

Fig. 1. Workflow for investigating the influence of key aspects of an MKO pipeline on residual error and joint angles. Experimental data (reference trajectory with soft tissue artefacts added to markers) is used as input to the pipeline. The impact of joint constraints is investigated by incorporating underlying models with differing joint constraints. Impact of errors during scaling (marker registration errors and segment scaling errors) are investigated. Markers (LASI: Left anterior superior iliac spine, RASI: Right anterior superior iliac spine, LPSIS: Left posterior superior iliac spine, RPSIS: Right posterior superior iliac spine, LTH1, LTH2, LTH3: Left lateral thigh cluster, LKNE: Left lateral femoral epicondyle, LTTB: Left tibial tuberosity, LSHN1, LTIB : Left shank cluster, LANK: Left lateral malleolus, LHEE : Left posterior distal aspect of the heel, LTOE: Left forefoot, LD1MT: Left heads of first metatarsals, LD5MT: Left heads of fifth metatarsals) with different weights are analysed to understand their influence on residual error and joint angles.

between residual errors and kinematic errors. However, the validity of residual errors as a goodness-of-fit metric has been questioned, with some studies reporting lower kinematic errors for higher residual errors (Smale et al., 2017), significant changes in computed kinematics with no change in residual errors (Dunne et al., 2021) and conversely, no significant change in kinematics with significant variation in residual errors (Thouzé et al., 2016).

Whilst the availability of true bone movement — acquired using intracortical pins, fluoroscopy or magnetic resonance imaging — has reduced kinematic uncertainty (Andersen et al., 2010), acquiring true bone movement is often impractical, thereby necessitating the need for a viable metric to evaluate the fidelity of computed kinematics. This need is further underscored by evidence that uncertainty in computed kinematics can significantly affect the reliability of subsequent biomechanical analysis (Muller et al., 2017; Myers et al., 2015; Ojeda et al., 2016).

In this study we aim to further ascertain the viability of using residual errors as a goodness-of-fit metric. Specifically, we investigate: (1) The impact of the MKO pipeline (segment scaling, marker registration, marker weights and joint models) on residual errors [Fig. 1]; and (2) The existence of a consistent causal relationship between residual errors and kinematic errors. We hypothesise that: (1) Residual errors are influenced by changes to any step of the MKO pipeline, albeit with varying impacts; and (2) Significant variations in residual errors from the reference leads to significant variations in joint angles, supporting the existence of a causal relationship. We believe our investigation will further the discussion on the validity and usability of residual errors as a goodness-of-fit metric, particularly in the absence of true bone movement.

2. Methods

2.1. Experimental data

Data used in this study were taken from Lamberto et al. (2017) and include both reference marker trajectories and 500 STA-affected marker trajectories of a single gait cycle. STA were added to the reference marker trajectories using STA models. Briefly, STA models for markers on the pelvis, shank, foot and lateral epicondyle were sinusoidal functions of time with amplitudes varied non-uniformly. STA models for the thigh markers were linear functions of hip and knee angles, with mean values derived from literature Bonci et al. (2014).

2.2. Baseline model and MKO framework

The baseline model used was a 4-segment model (pelvis, thigh, shank and foot) with three joints (hip, knee and ankle). The baseline model was based on the musculoskeletal model, gait2354, in OpenSim (Yamaguchi and Zajac, 1989) and contains an articulated joint with three degrees of freedom (DoF) for the hip, a coupling joint for the knee, and a joint with one DoF for the ankle. The baseline model was scaled based on the static trial provided, with scaling errors below the guidelines recommended by OpenSim (Root mean square error [RMSE] < 1 cm and maximum marker error < 2 cm).

To analyse the impact of each step of the MKO pipeline on residual errors, models differing from the baseline model were created to emulate possible errors/variations at each step of the pipeline. Joint angles and total residual errors for the 501 trajectories (500 STA-affected trajectories and the reference marker trajectories) were calculated for every model using the inverse kinematic (IK) analysis in OpenSim. All markers for the IK analyses were given an equal weight of 1 unless specified.

2.3. Model generation

2.3.1. Models with marker registration errors and segment scaling errors

Models emulating errors during the marker registration and segment scaling steps were created following the pipeline outlined by Uchida and Seth (2022). Briefly, models emulating marker registration errors were created by altering the marker location (in the segment coordinate system) of the baseline model by adding a random perturbation. The models were verified to confirm that the new location of each marker was within a maximum allowable deviation from its original position. To simulate segment scaling errors, models differing from the baseline model only in their scale factors were generated. For each model, the scale factors for every segment were selected at random from the range [90%-110%] of the baseline scale factors. The model was posed using IK to verify that each marker on the new model was within the maximum allowable deviation (stated below) from its original position.

Three models of increasing maximum allowable deviation (d) were generated for each error. Maximum allowable deviation of $d < 0.5$ cm, $0.5\text{ cm} < d < 1.25$ cm and $1.25\text{ cm} < d < 2$ cm were chosen as thresholds to reflect human-error during the processes.

Table 1
Marker acronyms and their respective names.

Marker label	Marker names
LASI	Left anterior superior iliac spine
RASI	Right anterior superior iliac spine
LPSIS	Left posterior superior iliac spine
RPSIS	Right posterior superior iliac spine
LTH1	Left lateral thigh cluster
LTH2	Left lateral thigh cluster
LTH3	Left lateral thigh cluster
LKNE	Left lateral knee epicondlyle
LTTB	Left tibial tuberosity
LSHN1	Left shank cluster
LTIB	Left shank cluster
LANK	Left lateral malleolus
LHEE	Left posterior distal aspect of the heel
LTOE	Left forefoot
LD1MT	Left head of first metatarsal
LD5MT	Left head of fifth metatarsal

2.3.2. Models with different marker weightings

Three marker weighting strategies were chosen. Weighting Strategy 1 (WS1), where all markers are given an equal weight of 1 (Fiorentino et al., 2020). Weighting strategy 2 (WS2), where anatomical landmarks are up-weighted (weight=5) with thigh and shank markers given a weight of 1 (Andersen et al., 2009). Weighting strategy 3 (WS3), where thigh markers are excluded and the remaining markers are given a weight of 1 (Bakke and Besier, 2022; Slater et al., 2018). Marker names are listed in Table 1.

2.3.3. Differing joint models

Two models incorporating joints with differing DoF to that of the baseline model were created. The first model (Ball) had articulated joints at the hip, knee and ankle, and the second model (6 DoF) considered every segment to be a free body.

2.4. Data comparison and statistical analysis

Total residual errors of each of the models were compared with that of the baseline model. One-way repeated measures analysis of variance (ANOVA) tests (significance level 0.05) were performed to investigate the effect of the MKO pipeline on residual errors. Post-hoc analyses using paired *t*-tests were performed with a corrected significance level based on Bonferroni corrections. Joint angles computed using each model were compared with that of the baseline model. Comparisons between joint angles were performed using paired *t*-tests (significance level 0.05). Additionally, a regression analysis between joint angle errors at every frame and mean total residual errors was performed.

For every significant result, Cohen's d effect sizes were calculated to determine the significance. For all tests, Cohen's d of 0.2 was considered small, 0.5 medium and > 0.8 large; Cohen's d was only calculated for frames with significant differences.

ANOVAs, paired *t*-tests and regression analyses were performed using statistical parametric mapping (SPM, (Pataky et al., 2013, 2015)). SPM utilises the entire one-dimensional time series data to make probabilistic inferences. Non-parametric tests were conducted if normality could not be assumed; normality tests in SPM were performed using the D'Agostino-Pearson K2 test.

3. Results

Our results indicate that every step of the MKO pipeline (marker registration, segment scaling, marker weights and joint models) had a significant effect on computed residual errors. For the sake of brevity, only cases for which at least one variation had a large effect size (Cohen's d > 0.8) are discussed; additional results and instructions on how to read SPM figures are available in Supplementary data.

3.1. Impact of MKO pipeline on residual errors

Errors in the marker registration step of the MKO pipeline had a significant effect on total residual errors (F = 4.744, p = 0.001, ANOVA; Fig. 2 I) as indicated by the one-way repeated measures ANOVA test. Total residual errors computed using the 3 models (models with increasing magnitudes of marker registration error) emulating errors in the marker registration step were greater than that of the baseline model for the entire duration of the gait cycle (p = 0.001, paired *t*-tests; Fig. 2 II a–c). Cohen's d indicated a large effect for the model with marker registration errors > 0.5 cm and < 1.25 cm at frames 1–20 and 40–113; and for the model with marker registration error > 1.25 cm and < 2 cm for the entire duration of the gait cycle (Fig. 2 II d). Median total residual errors were greater for the three models compared to the baseline model (Fig. 2 III).

Joint models incorporated in the model also had a significant impact on the total residual errors (F = 5.654,p = 0.001, ANOVA; Fig. 3 I). The Ball model (spherical constraints) had the greatest residual errors (p = 0.001, paired *t*-tests; Fig. 3 II a,c), and the baseline model had greater residual errors than the 6 DoF model (p = 0.001, paired *t*-tests; Fig. 3 II b). Cohen's d indicated large effects between the baseline and 6 DoF model and between the Ball and 6 DoF model for the entire duration of the gait cycle, with large effects observed at frames 1–22 and 42–113 between baseline and Ball model (Fig. 3 II d).

Despite segment scaling errors and marker weighting strategies having a significant impact on computed residual errors (F = 4.768, p = 0.001, ANOVA), none of the differences had a large effect size (Cohen's d < 0.8; Supplementary data).

3.2. Relationship between residual errors and joint angles

Joint angles computed using each of the models with marker registration errors differed significantly from those of the baseline model (p = 0.001, paired *t*-tests; Fig. 4 a–o). Large effect sizes were indicated by Cohen's d for the model with maximum marker registration error > 0.5 cm and < 1 .25 cm for hip rotation angle (frames 45–90; Fig. 4 q), and for ankle flexion angle (entire gait cycle; Fig. 4 t); and for the model with maximum marker registration error > 1.25 cm and < 2 cm for hip rotation angle (frames 1–8 and 50–113; Fig. 4 q), for hip adduction angle (frames 18–23; Fig. 4 r), for knee flexion angle (frames 20–25; Fig. 4 s) and for ankle flexion angle (entire gait cycle; Fig. 4 t).

Similarly, kinematics obtained using models with differing joint models varied significantly from one another (p = 0.001, paired *t*-tests; Fig. 5 a–o). Large effect sizes (Cohen's d > 0.8) were observed between the baseline and Ball models for hip flexion angles (frames 38–58; Fig. 5 p), hip rotation angles (entire gait cycle; Fig. 5 q), knee flexion angles (frames 10–82; Fig. 5 s) and ankle flexion angles (entire gait cycle; Fig. 5 t). Large effect sizes were also observed between the Ball and 6 DoF models for ankle flexion angle (frames 20–46; Fig. 5 t).

The results of a regression analysis between total residual errors and joint angle errors indicated significant positive correlations between: hip flexion angle errors and total residual errors (frames 48–53, 68–72;p = 0.0116,p = 0.0116; Fig. 6 a), hip adduction angle errors and total residual errors (frames 71–76;p = 0.0151; Fig. 6 c), knee flexion angle errors and total residual errors (frames 5–9, 48–60 and 80–86;p = 0.006,p = 0.0026,p = 0.006; Fig. 6 d) and between ankle angle errors and total residual errors (frames 32–87;p = 0.002; Fig. 6 e).

4. Discussion

In this study we aimed to further ascertain the validity of residual errors as a goodness-of-fit metric. Our results indicate that changes in the MKO pipeline result in significant variation in residual errors, which leads to significant changes in computed joint angles. These findings support the existence of a causal relationship between residual errors and joint angle errors.

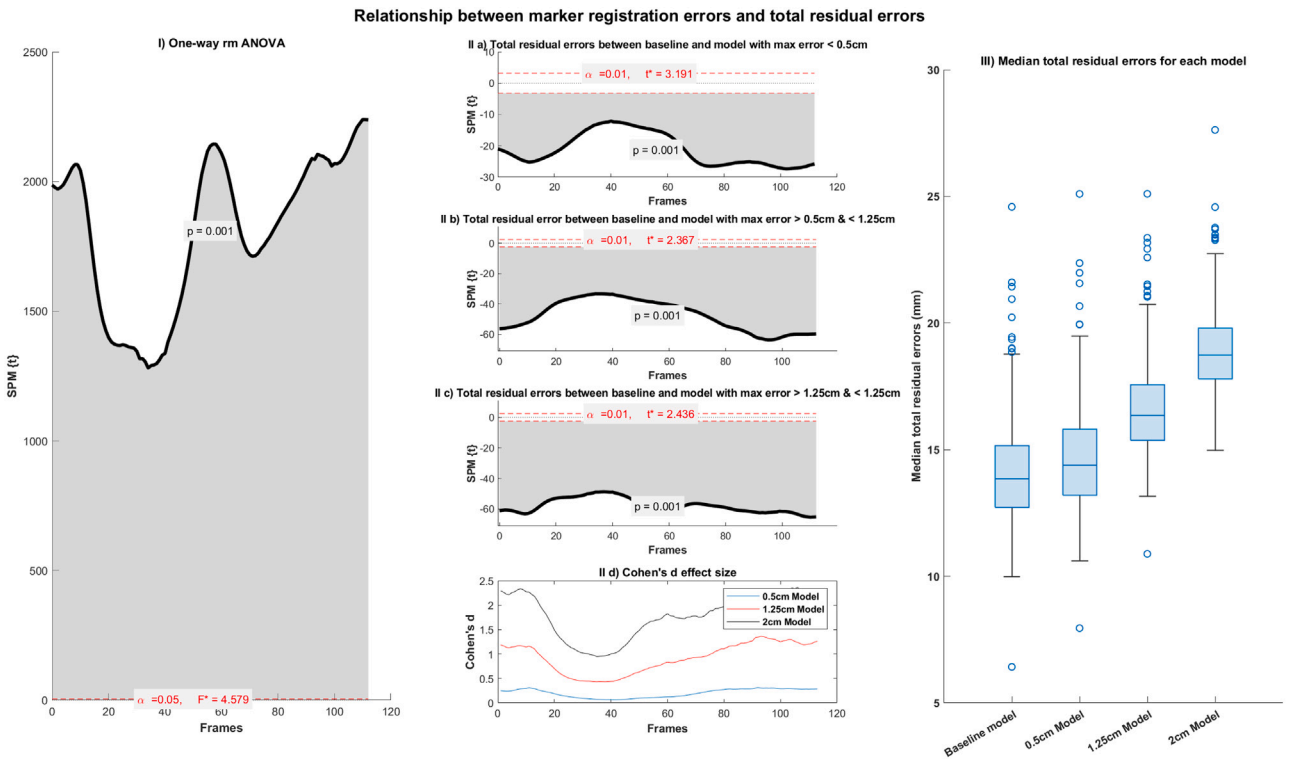

Fig. 2. (I) Results of a nonparametric one-way repeated measures ANOVA analysis between total residual errors acquired using the baseline model and three models with marker registration errors. The shaded area indicates marker registration has a significant effect on total residual errors (p = 0.001). (II) (a–c) Results of the post-hoc analyses using paired *t*-tests in SPM between total residual errors acquired using the baseline model and each of the models with marker registration errors. The shaded area shows a significant difference (p = 0.001) in total residual errors with models with marker registration errors having statistically greater total residual errors. (d) Cohen's d effect sizes between baseline model and three models with marker registration errors. (III) The box plot shows the median total residual error between the four models.

Marker registration and segment scaling are key steps in the MKO pipeline. Uchida and Seth (2022) reported that errors in these steps lead to variation in computed peak joint angles; however, they observed no effect on marker residual errors. Contrasting this, our results indicate that errors in these steps lead to a 35% increase in residual errors ($p < 0.05$; paired *t*-tests) with large effect sizes observed for errors in marker registration. Discrepancies between our and their results is likely attributable to differences in marker residual calculations. Specifically, they computed marker residuals as the RMSE difference between model-derived marker locations in their uncertainty-generated model and their baseline model, whilst ours were computed as the RMSE difference between model-derived marker position and input data.

Our findings, specifically the effect of marker registration errors, are similar to other studies investigating scaling methods. We leveraged a marker-based segment scaling and optimisation-based marker registration method, with both employing a static trial. One study comparing five scaling methods indicated that the scaling pipeline used in our investigation, albeit with dynamic trials, produced both the lowest residual errors and kinematics similar to that of reference kinematics. Additionally, they indicated that optimising segment lengths resulted in over-fitting of the model, with marker registration having a greater effect on residual errors and joint angles (Puchaud et al., 2020).

Conversely, another study comparing three scaling methods reported that no method was superior over another, with similar saggital kinematics obtained for all three methods and similar residual errors computed for the linear and kinematic scaling methods (Lund et al., 2015). Key differences in our study compared with the above are: the use of SPM, the analysis of the effect of errors in the scaling pipeline, and the use of static trials. We hypothesise that leveraging SPM and exploring the effects of errors might elucidate which scaling pipeline is superior. However, we believe using standing trials are the clinical standard, with functional trials infeasible for most clinical populations.

Marker weightings are used to reduce the impact of markers more prone to STA on computed kinematics, with marker weighting leveraged to reduce dynamic residuals. Although up-weighting anatomical markers or determining subject-and task-specific optimal marker weights have been recommended (Lefebvre et al., 2023; Begon et al., 2015), none of these studies have analysed the variation in residual errors due to different weighting strategies. Our results indicate that up-weighting anatomical markers (WS2) resulted in the greatest residual errors, whilst assigning markers with equal weights (WS1) resulted in the least residual errors (13.5 mm). However, the effect sizes were only small to moderate.

Constraints and joint models are an integral part of the MKO pipeline, with residual errors leveraged as a metric to investigate the effect of various constraints on the MKO pipeline. For example, soft, hard and loop closure constraints were found to increase residual errors in both kalman filter (KF)- and global optimisation (GO)-based MKO methods (Fohanno et al., 2014), with loop closures found to affect residual errors when the constraint formulation was modified to a penalty-based formulation (Livet et al., 2023). Similarly, one study reported a reduction in residual errors when an STA model was added in the constraint equation (Bonnet et al., 2017a) for both KF- and GO-formulations.

However, despite studies investigating the effect of differing joint models on computed kinematics (Richard et al., 2017; Duprey et al., 2010; Gasparutto et al., 2015), none have investigated the variation in residual errors. Our results indicate that joint model types have a significant ($p < 0.05$; one-way repeated measures ANOVA) effect on computed residual errors, with the least residual errors obtained for the 6 DoF model (11 mm) and the Ball model resulting in the greatest residual errors (17 mm). These results are in-line with findings reported by (Pomarat et al., 2023), who observed that the lowest residual errors were obtained for a model incorporating 6 DoF joints.

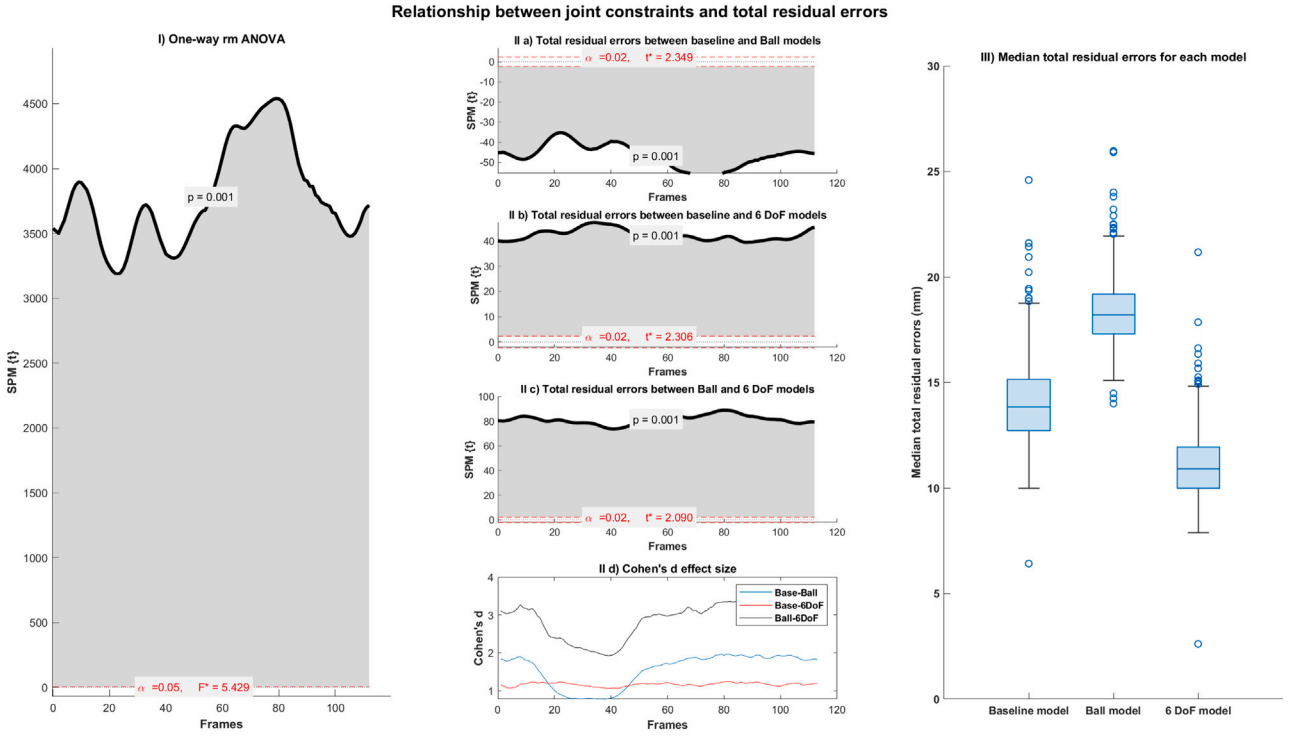

Fig. 3. (I) Results of a nonparametric one-way ANOVA analysis between total residual errors acquired using the three models. The shaded area indicates the choice of joint constraints have a significant effect on total residual errors (p = 0.001). (II) Post-hoc analyses using paired *t*-test in SPM between total residual errors acquired using each of the models. (a) Results indicate that the Ball model had significantly greater total residual (p = 0.001) errors compared to the baseline model. MeanA is the baseline model and meanB is the Ball model. (b) The shaded area shows that the baseline model had statistically higher (p = 0.001) total residual errors compared to the 6 DoF model. MeanA is the baseline model and meanB is 6 DoF model. (c) The plot indicates that total residual errors for the Ball model were significantly higher (p = 0.001) than those for the 6 DoF model. MeanA is the Ball model and meanB is the 6 DoF model. (d) Cohen's d effect sizes between baseline, Ball and 6DoF models. (III) The box plot shows the median total residual errors acquired using the three models.

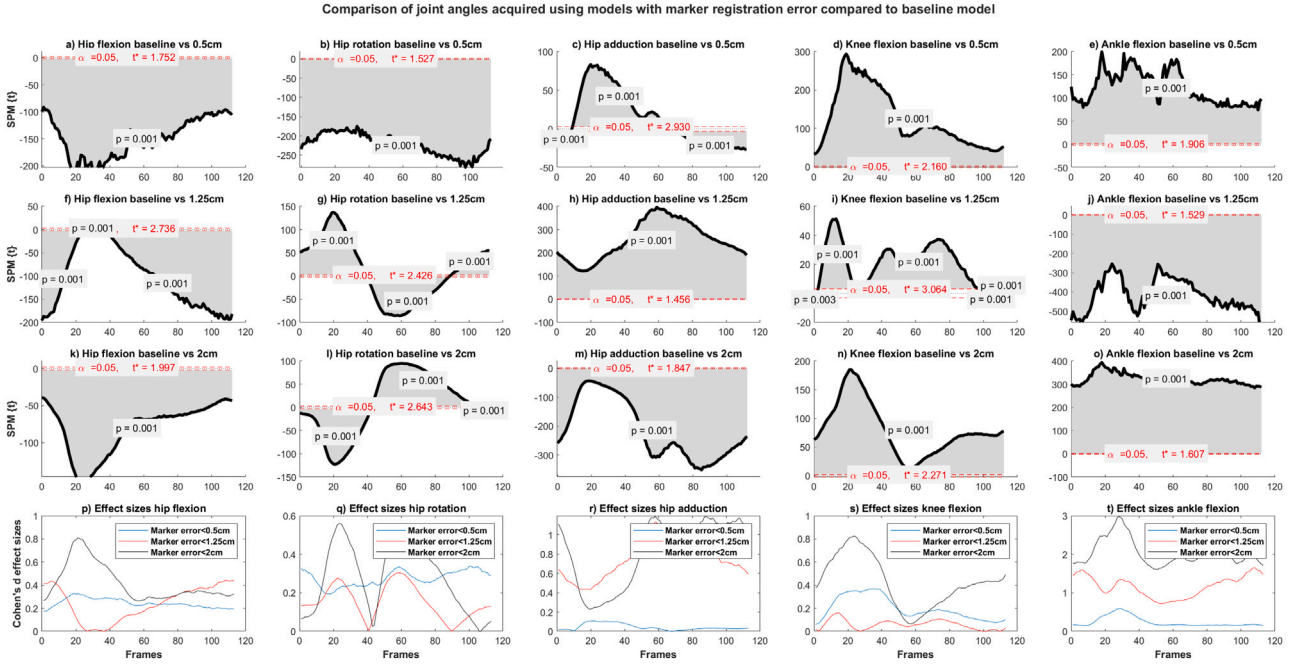

Fig. 4. (a–e) Paired *t*-tests between joint angles acquired using baseline model and model with maximum marker error of < 0.5 cm. Shaded region indicates significant variation in joint angles (p = 0.001). (f–j) Paired *t*-tests between joint angles acquired using baseline model and model with maximum marker error of < 1.25 cm with shaded region indicating significant variation between joint angles (p = 0.001). (k–o) Paired *t*-tests between joint angles acquired using baseline model and model with maximum marker error of < 2 cm. Shaded region indicates significant variation in joint angles (p = 0.001). (p–t) Cohen's d effect sizes between the three models for hip flexion, hip rotation, hip adduction, knee flexion and ankle flexion. The columns are for hip flexion, hip rotation, hip adduction, knee flexion and ankle flexion joint angles respectively.

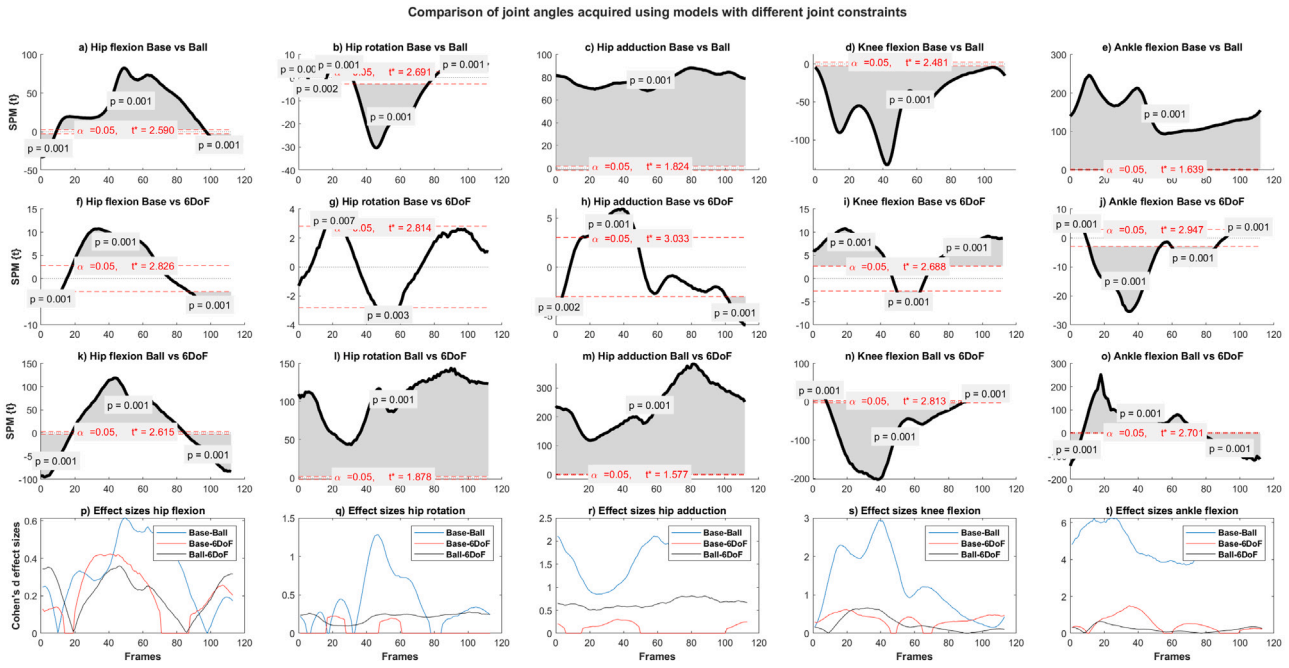

Fig. 5. (a–e) Paired t-tests between joint angles acquired using the baseline model and Ball model. Shaded region indicates significant variation in joint angles (p = 0.001). MeanA was the baseline model and meanB the Ball model. (f–j) Paired t-tests between joint angles acquired using the baseline model and 6 DoF model with results indicating significant variation between joint angles (p = 0.001). MeanA was the baseline model and meanB the 6 DoF model. (k–o) Paired t-tests between joint angles acquired using the Ball model and 6 DoF model. Shaded region indicates significant variation in joint angles (p = 0.001). MeanA was the Ball model and meanB the 6 DoF model. (p–t) Cohen's d effect sizes between the three models for hip flexion, hip rotation, hip adduction, knee flexion and ankle flexion. The columns are for hip flexion, hip rotation, hip adduction, knee flexion and ankle flexion joint angles respectively.

Whilst our investigation does not incorporate additional constraints, and our joint models were defined using mobilisers (Seth et al., 2010), we hypothesise (based on our results and the aforementioned studies) that different formulations of joint types would affect residual errors, with the addition of any constraints having a significant impact on residual errors.

The above results indicate that every step of the MKO pipeline has a significant effect on computed residual errors. Mathematically, residual errors and joint angles are linked (with optimal joint angles obtained for lower residual errors), supporting a causal relationship. Therefore, variations in residual errors due to the MKO pipeline may indicate uncertainties in computed kinematics, and could result in misclassification of pathologies (Steele et al., 2013) or affect subsequent analyses. Uncertainties in kinematics have been reported to affect moment calculation, forces and muscle activation, with uncertainties in kinematics found to contribute more to dynamic residuals than uncertainties in force plate data (Muller et al., 2017).

Despite the mathematical relationship, studies have questioned the existence of a causal relationship between residual errors and joint angles. However, our results indicated that significant ($p < 0.05$; paired t-tests) variations in residual errors from the baseline were generally reflected in significantly ($p < 0.05$; paired t-tests) different computed joint angles. Furthermore, large effect sizes in residual error variation resulted in large effect sizes in joint angle variation. Additionally, the regression analysis indicated that when employing the same MKO pipeline, increases in residual errors were positively correlated with increases in ankle flexion, hip flexion, hip adduction and knee flexion joint angle errors. These two results (variation and regression analysis) support the existence of a causal relationship between residual errors and joint angle errors.

Although our results support the existence of a causal relationship, a consistent causal relationship could not be established. Whilst variations of large effect sizes in residual errors typically resulted in variations of large effect sizes in joint angles, their relationship was not consistently one-to-one at every frame. Additionally, effect sizes varied between joint angles and large effect sizes in joint angle variation were observed for small to moderate variations in residual errors (Supplementary data).

The above findings are echoed in other studies. For example, whilst incorporating an STA model in the MKO pipeline resulted in smaller residual errors, only the formulation leveraging KF had a subsequent decrease in joint angle errors (Bonnet et al., 2017a). Similarly, differing marker sets reported similar residual errors for different joint angles (Fohanno et al., 2015). The inconsistent causal relationship reported in both our results and these results could be attributed to the MKO formulation, where the least-squares minimisation problem can cause a local minima, resulting in different kinematics depending on the initial state. This can be visualised in Fig. 4 p, wherein the effect of differing marker registration errors results in differing effect sizes and joint angles across the gait cycle. This can be attributed to the algorithm spreading the marker error to find optimal joint angles, which could result in a local minima at every frame.

The general finding of a causal relationship and the nonlinear behaviour shown in our results can be attributed to us leveraging the entire time-series data, rather than data condensed to a singular value. Information may be lost when analysing time-series data using a single value, leading to obscuring of variations and patterns. For example, greater residual errors with moderate effect sizes would not be observed by condensing residual errors to a single value [box plots, (Fig. 2 III)]. Additionally, despite significant variations reported in both joint angles and residual error variations using SPM, regression analyses using mean residual error values (scalar) could not capture the variation.

The above inconsistency could also be affected by the two main limitations of this study. Firstly, joint angle errors are relative errors and are dependent on the baseline data, which also produces residual errors. Secondly, residual errors caused by individual steps of the MKO pipeline could not be decoupled, leading to the nonlinear relationship and the resulting complex interplay between residual errors and joint angle errors.

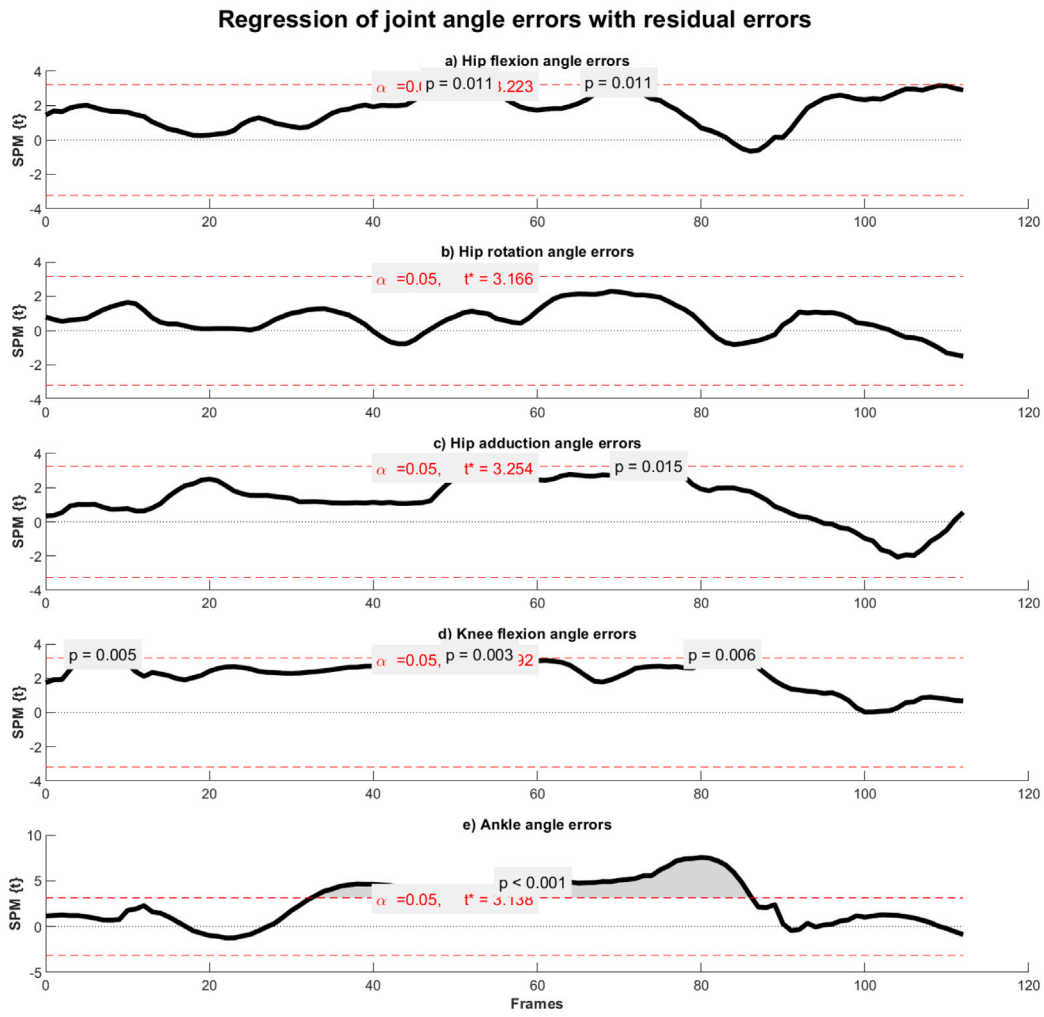

Fig. 6. How to read SPM figures: The red lines indicate the critical threshold set at the respective alpha values (0.05 for regression tests). For regression tests if the t-statistic field vector transverse the critical threshold (shaded region), the null hypothesis of no relationship is rejected. For regression analyses, if the t-statistic field vector transverses the upper critical threshold, then there is a positive relationship between continuous variable (joint angle errors) and discrete variable (median total residual errors) and vice versa if it transverses the lower critical threshold.
Regression analysis between joint angle errors and total residual errors for: (a) hip flexion angle errors. (b) hip adduction angle errors. (c) hip rotation angle errors. (d) knee flexion angle errors. (e) ankle angle errors. The shaded regions show statistically significant positive correlations. (For interpretation of the references to colour in this figure legend, the reader is referred to the web version of this article.)

Whilst the validity of both MKO methods and residual errors are still being questioned, with multiple studies leveraging true bone movement obtained from intracortical pins, percutaneous trackers or imaging modalities (Holden et al., 1997) to reduce kinematic uncertainty, acquiring true bone movement is impractical in most settings. Therefore, residual errors are often leveraged as a goodness-of-fit metric. In this study we have observed that every step of the MKO pipeline has a significant but varying effect on computed residual errors, which in turn has a significant effect on computed joint angles. The above findings were obtained by leveraging time-series analysis using SPM over scalar approaches.

In conclusion, our results strongly support the existence of an inconsistent causal relationship between residual errors and kinematic errors, and underscore the need to leverage time-series statistics over scalar approaches.

CRediT authorship contribution statement

Vignesh Radhakrishnan: Writing – review & editing, Writing – original draft, Visualization, Validation, Software, Resources, Methodology, Investigation, Formal analysis, Data curation, Conceptualization. **Samadhan Patil:** Writing – review & editing, Validation, Supervision, Resources, Project administration. **Adar Pelah:** Writing – review & editing, Writing – original draft, Validation, Supervision, Resources, Project administration. **Peter Ellison:** Writing – review & editing, Writing – original draft, Validation, Supervision, Project administration.

Declaration of competing interest

All authors declare that there are no conflicts of interest.

Acknowledgements

We would like to thank the creators of Statistical parametric mapping (SPM) for their prompt response in answering queries and for providing the software (spm1d), (Pataky, 2010) No additional sources of funding were utilised in this research.

Appendix A. Supplementary data

Supplementary material related to this article can be found online at https://doi.org/10.1016/j.jbiomech.2024.112395.

References

Andersen, M.S., Benoit, D.L., Damsgaard, M., Ramsey, D.K., Rasmussen, J., 2010. Do kinematic models reduce the effects of soft tissue artefacts in skin marker-based motion analysis? An in vivo study of knee kinematics. J. Biomech. 43 (2), 268–273.

Andersen, M.S., Damsgaard, M., Rasmussen, J., 2009. Kinematic analysis of over-determinate biomechanical systems. Comput. Methods Biomech. Biomed. Eng. 12 (4), 371–384.

Andersen, M.S., Damsgaard, M., Rasmussen, J., Ramsey, D.K., Benoit, D.L., 2012. A linear soft tissue artefact model for human movement analysis: proof of concept using in vivo data. Gait Posture 35 (4), 606–611.

Bakke, D., Besier, T., 2022. Shape-model scaled gait models can neglect segment markers without consequential change to inverse kinematics results. J. Biomech. 137 (111086), 111086.

Begon, M., Andersen, M.S., Dumas, R., 2018. Multibody kinematics optimization for the estimation of upper and lower limb human joint kinematics: A systematized methodological review. J. Biomech. Eng. 140 (3).

Begon, M., Dal Maso, F., Arndt, A., Monnet, T., 2015. Can optimal marker weightings improve thoracohumeral kinematics accuracy? J. Biomech. 48 (10), 2019–2025.

Bonci, T., Camomilla, V., Dumas, R., Chèze, L., Cappozzo, A., 2014. A soft tissue artefact model driven by proximal and distal joint kinematics. J. Biomech. 47 (10), 2354–2361.

Bonnet, V., Dumas, R., Cappozzo, A., Joukov, V., Daune, G., Kulić, D., Fraisse, P., Andary, S., Venture, G., 2017a. A constrained extended Kalman filter for the optimal estimate of kinematics and kinetics of a sagittal symmetric exercise. J. Biomech. 62, 140–147.

Bonnet, V., Richard, V., Camomilla, V., Venture, G., Cappozzo, A., Dumas, R., 2017b. Joint kinematics estimation using a multi-body kinematics optimisation and an extended Kalman filter, and embedding a soft tissue artefact model. J. Biomech. 62, 148–155.

Camomilla, V., Bonci, T., Cappozzo, A., 2017. Soft tissue displacement over pelvic anatomical landmarks during 3-D hip movements. J. Biomech. 62, 14–20.

Cappello, A., Stagni, R., Fantozzi, S., Leardini, A., 2005. Soft tissue artifact compensation in knee kinematics by double anatomical landmark calibration: performance of a novel method during selected motor tasks. IEEE Trans. Biomed. Eng. 52 (6), 992–998.

Damsgaard, M., Rasmussen, J., Christensen, S.T., Surma, E., de Zee, M., 2006. Analysis of musculoskeletal systems in the anybody modeling system. Simul. Model. Pract. Theory 14 (8), 1100–1111.

De Groote, F., De Laet, T., Jonkers, I., De Schutter, J., 2008. Kalman smoothing improves the estimation of joint kinematics and kinetics in marker-based human gait analysis. J. Biomech. 41 (16), 3390–3398.

Delp, S.L., Anderson, F.C., Arnold, A.S., Loan, P., Habib, A., John, C.T., Guendelman, E., Thelen, D.G., 2007. OpenSim: open-source software to create and analyze dynamic simulations of movement. IEEE Trans. Biomed. Eng. 54 (11), 1940–1950.

Dunne, J.J., Uchida, T.K., Besier, T.F., Delp, S.L., Seth, A., 2021. A marker registration method to improve joint angles computed by constrained inverse kinematics. PLoS One 16 (5), e0252425.

Duprey, S., Cheze, L., Dumas, R., 2010. Influence of joint constraints on lower limb kinematics estimation from skin markers using global optimization. J. Biomech. 43 (14), 2858–2862.

Fiorentino, N.M., Atkins, P.R., Kutschke, M.J., Bo Foreman, K., Anderson, A.E., 2020. Soft tissue artifact causes underestimation of hip joint kinematics and kinetics in a rigid-body musculoskeletal model. J. Biomech. 108 (109890), 109890.

Fohanno, V., Begon, M., Lacouture, P., Colloud, F., 2014. Estimating joint kinematics of a whole body chain model with closed-loop constraints. Multibody Syst. Dyn. 31 (4), 433–449.

Fohanno, V., Lacouture, P., Colloud, F., 2015. Influence of the marker set on the reconstruction of the whole-body kinematics. Mov. Sport Sci. 90 (90), 29–36.

Gasparutto, X., Sancisi, N., Jacquelin, E., Parenti-Castelli, V., Dumas, R., 2015. Validation of a multi-body optimization with knee kinematic models including ligament constraints. J. Biomech. 48 (6), 1141–1146.

Holden, J.P., Orsini, J.A., Siegel, K.L., Kepple, T.M., Gerber, L.H., Stanhope, S.J., 1997. Surface movement errors in shank kinematics and knee kinetics during gait. Gait Posture 5 (3), 217–227.

Kainz, H., Modenese, L., Lloyd, D.G., Maine, S., Walsh, H.P.J., Carty, C.P., 2016. Joint kinematic calculation based on clinical direct kinematic versus inverse kinematic gait models. J. Biomech. 49 (9), 1658–1669.

Laitenberger, M., Raison, M., Périé, D., Begon, M., 2015. Refinement of the upper limb joint kinematics and dynamics using a subject-specific closed-loop forearm model. Multibody Syst. Dyn. 33 (4), 413–438.

Lamberto, G., Martelli, S., Cappozzo, A., Mazzà, C., 2017. To what extent is joint and muscle mechanics predicted by musculoskeletal models sensitive to soft tissue artefacts? J. Biomech. 62, 68–76.

Leardini, A., Chiari, L., Della Croce, U., Cappozzo, A., 2005. Human movement analysis using stereophotogrammetry. Part 3. Soft tissue artifact assessment and compensation. Gait Posture 21 (2), 212–225.

Lefebvre, F., Rogowski, I., Long, N., Blache, Y., 2023. Influence of marker weights optimization on scapular kinematics estimated with a multibody kinematic optimization. J. Biomech. 159 (111795), 111795.

Livet, C., Rouvier, T., Sauret, C., Pillet, H., Dumont, G., Pontonnier, C., 2023. A penalty method for constrained multibody kinematics optimisation using a Levenberg-Marquardt algorithm. Comput. Methods Biomech. Biomed. Eng. 26 (7), 864–875.

Lu, T.W., O'Connor, J.J., 1999. Bone position estimation from skin marker co-ordinates using global optimisation with joint constraints. J. Biomech. 32 (2), 129–134.

Lund, M.E., Andersen, M.S., de Zee, M., Rasmussen, J., 2015. Scaling of musculoskeletal models from static and dynamic trials. Int. Biomech. 2 (1), 1–11.

Muller, A., Pontonnier, C., Dumont, G., 2017. Uncertainty propagation in multibody human model dynamics. Multibody Syst. Dyn. 40 (2), 177–192.

Myers, C.A., Laz, P.J., Shelburne, K.B., Davidson, B.S., 2015. A probabilistic approach to quantify the impact of uncertainty propagation in musculoskeletal simulations. Ann. Biomed. Eng. 43 (5), 1098–1111.

Ojeda, J., Martínez-Reina, J., Mayo, J., 2014. A method to evaluate human skeletal models using marker residuals and global optimization. Mech. Mach. Theory 73, 259–272.

Ojeda, J., Martínez-Reina, J., Mayo, J., 2016. The effect of kinematic constraints in the inverse dynamics problem in biomechanics. Multibody Syst. Dyn. 37 (3), 291–309.

Pataky, T.C., 2010. Generalized n-dimensional biomechanical field analysis using statistical parametric mapping. J. Biomech. 43 (10), 1976–1982.

Pataky, T.C., Robinson, M.A., Vanrenterghem, J., 2013. Vector field statistical analysis of kinematic and force trajectories. J. Biomech. 46 (14), 2394–2401.

Pataky, T.C., Vanrenterghem, J., Robinson, M.A., 2015. Zero- vs. one-dimensional, parametric vs. non-parametric, and confidence interval vs. hypothesis testing procedures in one-dimensional biomechanical trajectory analysis. J. Biomech. 48 (7), 1277–1285.

Pomarat, Z., Guitteny, S., Dumas, R., Muller, A., 2023. Kinetics influence of multibody kinematics optimisation for soft tissue artefact compensation. J. Biomech. 150 (111514), 111514.

Puchaud, P., Sauret, C., Muller, A., Bideau, N., Dumont, G., Pillet, H., Pontonnier, C., 2020. Accuracy and kinematics consistency of marker-based scaling approaches on a lower limb model: a comparative study with imagery data. Comput. Methods Biomech. Biomed. Eng. 23 (3), 114–125.

Richard, V., Cappozzo, A., Dumas, R., 2017. Comparative assessment of knee joint models used in multi-body kinematics optimisation for soft tissue artefact compensation. J. Biomech. 62, 95–101.

Seth, A., Sherman, M., Eastman, P., Delp, S., 2010. Minimal formulation of joint motion for biomechanisms. Nonlinear Dynam. 62 (1), 291–303.

Slater, A.A., Hullfish, T.J., Baxter, J.R., 2018. The impact of thigh and shank marker quantity on lower extremity kinematics using a constrained model. BMC Musculoskelet. Disord. 19 (1), 399.

Smale, K.B., Potvin, B.M., Shourijeh, M.S., Benoit, D.L., 2017. Knee joint kinematics and kinetics during the hop and cut after soft tissue artifact suppression: Time to reconsider ACL injury mechanisms? J. Biomech. 62, 132–139.

Steele, K.M., Seth, A., Hicks, J.L., Schwartz, M.H., Delp, S.L., 2013. Muscle contributions to vertical and fore-aft accelerations are altered in subjects with crouch gait. Gait Posture 38 (1), 86–91.

Thouzé, A., Monnet, T., Bélaise, C., Lacouture, P., Begon, M., 2016. A chain kinematic model to assess the movement of lower-limb including wobbling masses. Comput. Methods Biomech. Biomed. Eng. 19 (7), 707–716.

Uchida, T.K., Seth, A., 2022. Conclusion or illusion: Quantifying uncertainty in inverse analyses from marker-based motion capture due to errors in marker registration and model scaling. Front. Bioeng. Biotechnol. 10, 874725.

Yamaguchi, G.T., Zajac, F.E., 1989. A planar model of the knee joint to characterize the knee extensor mechanism. J. Biomech. 22 (1), 1–10.